Open Access

Shai Shefer, Alvaro Israel, Alexander Golberg[a] and Alexandra Chudnovsky[a,*]

Carbohydrate-based phenotyping of the green macroalga *Ulva fasciata* using near-infrared spectrometry: potential implications for marine biorefinery

DOI 10.1515/bot-2016-0039
Received 13 May, 2016; accepted 23 November, 2016; online first 13 January, 2017

Abstract: Marine macroalgal biomass is a promising sustainable feedstock for biorefineries. However, the development of macroalgal biomass for industrial cultivation and processing has been slow. In terrestrial plants, high-throughput phenotyping provides rapid imaging methods to select specimens with required properties, rapidly transforming traditional breeding techniques. To foster the development of macroalgal biomass for biorefinery applications, we developed a near-infrared spectrometry-based method for rapid phenotyping of the macroalga *Ulva fasciata* based on its glucose, rhamnose, xylose and glucuronic acid contents. Spectral slopes were calculated as indicative of major carbohydrate content change. In addition, different spectral indices were generated to distinguish between low and high contents of glucose, rhamnose, xylose and glucuronic acid in wet and dry biomass. Since glucose is a major monosaccharide in *Ulva* that is fermentable to bioethanol, as an example of future application, we developed a multivariate data analysis based on partial least squares regression to predict its content in dry and wet biomass samples solely from reflectance data. These methods could provide a useful, high-throughput tool to rapidly select thalli with high carbohydrate content for further propagation and to be used for feedstock development for marine biorefineries.

[a]**Alexander Golberg and Alexandra Chudnovsky:** These senior authors contributed equally to this work.
***Corresponding author: Alexandra Chudnovsky,** Department of Geography and Human Environment, Tel Aviv University, Zalig Street 10, Ramat Aviv, Tel Aviv 69978, Israel, e-mail: achudnov@post.tau.ac.il
Shai Shefer and Alexander Golberg: Porter School of Environmental Studies, Tel Aviv University, Tel Aviv, Israel
Alvaro Israel: Israel Oceanographic and Limnological Research Ltd., Haifa, Israel

Keywords: biorefinery; macroalga *Ulva*; near-infrared spectroscopy; phenotyping; single thallus cultivation.

Introduction

Biorefinery is a collective term for the complex system that includes biomass production, transportation, conversion into products and product distribution. Concerns over net energy balance, potable water use, environmental hazards and processing technologies call into question the potential for terrestrial biomass, such as cereal crops and lignocellulose biomass, to provide sustainable feedstock for biorefineries (Gerbens-Leenes et al. 2009). In addition, cost-effective cultivation and further processing difficulties currently prevent the implementation of large-scale microalgal technologies (Hannon et al. 2010). Alternatively, an expanding body of evidence has demonstrated that marine macroalgae can provide a sustainable alternative source of biomass for food, animal feed, fuel and production of chemicals (Bruhn et al. 2011, Wargacki et al. 2012, Kraan 2013, van der Wal et al. 2013, Aitken et al. 2014, Golberg et al. 2014). Green macroalgae from the genus *Ulva* are of particular interest because of their high growth rates and fermentable carbohydrate content (Golberg et al. 2014, Korzen et al. 2015a,b, Vitkin et al. 2015).

In addition to technological improvements needed for large-scale cultivation, significant effort is required to develop and select macroalgal species and strains with specific properties tailored for food, chemicals or fuel applications (Robinson et al. 2012). Industrial strain development in agricultural crops was transformed by the introduction of high-throughput phenotyping with imaging. Imaging methods, such as imaging spectroscopy, thermal infrared imaging, fluorescence imaging, 3D imaging and tomographic imaging, have been used to determine the required properties of plants for robust, cost-effective downstream processing (Cabrera-Bosquet

et al. 2012, Li et al. 2014, Mutka and Bart 2015, Walter et al. 2015). However, to the best of our knowledge, none of these methods have been used for macroalgal strain selection.

Near-infrared spectroscopy (NIRS) is a widely used technology with broad applications in virtually all fields of science (Blanco and Villarroya 2002) and has been extensively used for high-throughput breeding of plants. In macroalgae, spectral signatures based on absorption features can be used as indicative of the macroalgal type and condition (Ramsey et al. 2002a,b, Malta et al. 2003). Furthermore, thallus absorption in the visible (VIS) wavelength region is the optical feature most closely aligned with pigments and concentration changes (Ramsey et al. 2002a,b). Jiao and Liu (1999) proposed a simple spectrophotometric method to estimate microgram quantities of algal polysaccharide. The method was based on the binding of a dye to algal polysaccharides that causes the absorption maximum at 664 nm to decrease linearly over the range of 0–30 µg. In a previous NIRS work, Robic et al. (2009) developed a partial least squares (PLS) model to characterise the chemical composition of ulvan, a major polymer of *Ulva*, with functional properties making it interesting for industrial production. That work focused on determining the chemical composition of the extracted ulvan (Robic et al. 2009). However, to the best of our knowledge, NIRS has not been used for complete *Ulva* biomass phenotyping based on its content of major monosaccharides, which are critically important for the rapid selection of macroalgal feedstock for biofuel and biorefinery applications (Golberg et al. 2014, Korzen et al. 2015a,b, Vitkin et al. 2015).

The current study explored direct *Ulva* biomass phenotyping based on spectral slopes and spectral index analyses of monosaccharides. Specifically, we investigated the potential of NIRS to distinguish between low and high contents of glucose, rhamnose, xylose and glucuronic acid from fresh and dried tissues of *Ulva fasciata* L. based on the differences in the spectral signatures of thalli. We decided to focus on these molecules as they are the major carbohydrates in the *Ulva* species. In addition, in our previous work, we showed that the glucose, rhamnose and xylose contents of *U. fasciata* predict the potential of this feedstock for bioethanol fermentation (Vitkin et al. 2015). In addition to examining the potential use of reflectance spectroscopy for deriving different sugar contents, we developed PLS to predict the contents of specific monosaccharides based on whole thalli spectrum features. The methodology and tools developed in this study will facilitate the high-throughput phenotyping of macroalgal biomass, enabling its use as a major feedstock for sustainable biorefinery.

Materials and methods

Cultivation experiments

The model species used in this study was *Ulva fasciata* L., a green marine macroalga of worldwide distribution found in the intertidal and shallow waters within the Israeli Mediterranean shores. For the current study, specimens were taken from stocks maintained at a seaweed collection at Israel Oceanographic and Limnological Research, Haifa, Israel (IOLR). Cultivation trials were conducted in an outdoor setting at IOLR. One selected thallus was cut into 16 pieces, measuring approximately 5 cm^2 [weighing 0.4–0.6 g fresh weight (FW) each]. This single mother plant was used to produce 16 clones with identical genetic backgrounds needed for the comparative nature of this study. Single pieces were placed in 15×15-cm plastic net baskets. A total of 16 baskets, with a single thallus per basket, were divided into two groups, eight baskets each, and tied to 40-l fibreglass tanks supplied with running seawater and aeration. The first group of eight baskets was supplied with 1 mM NH_4Cl and 0.1 mM NaH_2PO_4 every week. With each nutrient application, the water exchange was stopped for 24 h to allow for absorption. The second group of eight baskets served as controls and had no nutrient supplements. The total cultivation time for both groups during March 2015 was 4 weeks under seawater temperatures ranging from 23 to 25°C and irradiances of 100–200 µmol photons m^{-2} s^{-1}. Each week, each thallus was weighed and returned to the basket. Growth rate was defined as the biomass accumulation for each of 16 thalli per week at the above-specified experimental conditions.

Drying and thermochemical hydrolysis

Following the growth period in the outdoor tanks, each thallus was dried separately at 60°C for 48 h until constant weight and ground into powder manually in a mortar with liquid nitrogen. For hydrolysis, 0.05 g of *Ulva fasciata* powder was mixed with 2 ml of sulphuric acid (5%) in 10-ml plastic tubes and autoclaved at 120°C for 45 min. Next, 500 mM phosphate buffer (Sigma, Israel) was added into the above mix and the resulting hydrolysate was neutralised with 3 M sodium hydroxide (NaOH) to pH 7.

Monosaccharide and sugar acid content determination with ion chromatography

Dionex ICS-5000 (Thermo Fischer Scientific, CA, USA) was used to quantify the monosaccharides glucose, rhamnose, xylose and glucuronic acid in the hydrolysates. Carbopac MA1 (Thermo Fischer Scientific, MA, USA) and its corresponding guard column were used for separation. An electrochemical detector with AgCl as reference electrode was used for detection. A trinary solvent system (Table 1) was used for elution. The column temperature was kept at 30°C and flow rate 0.25 ml min^{-1}. Calibration curves were made for rhamnose, glucose, xylose and glucuronic acid (0–100 μg ml^{-1}) to determine the concentration of corresponding substances in the hydrolysates.

Spectral reflectance measurements

Wet (n = 16) and dry (n = 16) samples, derived from the same initial thallus, were scanned by a Fieldspec Analytical Spectral Devices (ASD) full-range (FR) spectrometer (Analytical Spectral Devices, CO, USA) at three locations on each thallus. The FR spectrometer samples a spectral range of 350–2500 nm (http://www.asdi.com). The instrument uses three detectors spanning the visible, near-infrared (VNIR, comprising a Si photodiode array) and shortwave infrared (SWIR1 and SWIR2, comprising two separate InGaAs photodiodes). All samples were measured in the laboratory by attaching the high-intensity ASD contact probe ("potato") device to the sample and extracting an average of 40 readings, using bare fibre and self-probed illumination. The "potato" was set on a stable tripod base and maintained in a constant position at a nadir-looking angle. For all measurements, we used a Spectralon standard white reference panel (Spectralon, Labsphere Inc., www.labsphere.com) in the same geometry as a white reference to enable conversion of the measurement data into reflectance values.

Table 1: Ion chromatography elution protocol.

Time (min)	A (water)	B (250 mM NaOH)	C (1 M NaAcO)
0	94%	6%	0%
10	52	8	40
12	22	8	70
18	20	80	0
20	94	6	0

NIRS data analyses: slope and spectral index calculation

In this study, the spectral behaviour vs. chemical information on the wet and dry *Ulva* was visually inspected. The differences in spectral behaviour as a function of wavelength, which are indicative of changes in chemical properties, were identified. Importantly, the main criterion for spectral slope selection across the entire spectral range was similar for both wet and dry samples (Lugassi et al. 2015a,b). The slope was calculated using the following equation (Equation 1):

$$\text{Slope} = \frac{y_2 - y_1}{x_2 - x_1} \tag{1}$$

where the change in y signifies the change in spectral reflectance between two wavelengths and the change in x is the spectral range. We studied the dependence of spectral shape parameters on different sugar content distributions for all samples.

In addition, we calculated the normalised difference index (NDI) as follows:

$$\text{NDI} = \frac{R_{\lambda 1} - R_{\lambda 2}}{R_{\lambda 1} + R_{\lambda 2}} \tag{2}$$

where $R_{\lambda 1}$ and $R_{\lambda 2}$ are the values of spectral reflectance at two selected wavelengths. This index aims to identify the region of a rapid change in reflectance and to differentiate across the electromagnetic spectrum between *Ulva* thalli growth with and without external nutrient supply. To that end, the differences between two wavelengths were visually inspected and identified.

Feasibility of carbohydrate quantification in *Ulva* thalli using PLS

Partial least squares (PLS) regressions were run, with the goal being to define a relationship between different spectra and the concentration of each chemical constituent (e.g. rhamnose, xylose and glucuronic acid)

$$Y = A + A_1X_1 + A_2X_2 + A_3X_3 + \ldots\ldots + A_nX_n \tag{3}$$

where Y is the chemical constituent, A is an empirical coefficient and X_{1-n} are wavelengths.

Due to the limited number of samples (n = 16), leave-one-out cross-validation analyses (e.g. only one sample at a time is kept out of the calibration and used for prediction) were run (Mark 2000, Esbensen 2002). The difference between the predicted and measured carbohydrate

contents was expressed as a root mean square error of cross-validation (RMSECV). RMSECV is defined as the square root of the average of the squared differences between the predicted and measured values of the validation objects (Esbensen 2002):

$$\mathrm{RMSECV} = \left[\frac{\Sigma(X_m - X_p)^2}{n_v}\right]^{1/2} \quad (4)$$

where X_m is the chemically measured value of a sample, X_p is the predicted value of the sample on the basis of spectral analysis and n_v is the number of samples in the calibration stage. The accuracy of each calibration model was evaluated based on the coefficient of determination (R^2) for predicted vs. measured carbohydrate content in cross-validation and by slope. In addition, values of the ratio of prediction to deviation (RPD) were calculated to verify the applicability of the calibration (Williams and Norris 2001). RPD is defined as the ratio of the standard deviation of the *Y* values (e.g. sugar content) to the RMSECV (Mouazen et al. 2005). An RPD value was defined using the following ranges: 0–2 as not recommended and between 2.0 and 2.5 translated to mean that quantitative prediction is possible. RPD values above 3.0 were considered to indicate that the predictive capability of the model is excellent. Note, however, that the classification of RPD values of prediction accuracy slightly varies among different studies (Viscarra Rossel 2007).

To identify significant *X* variables, we ran Martens' uncertainty test (Unscrumbler, Version 9.1, Camo, Norway, 2004; Esbensen 2002). Therefore, we first ran our models on the whole wavelength region, and thereafter only significant wavelengths were kept and each model was reassessed using Martens' uncertainty test (Esbensen 2002). To simplify the spectral signals, thereby ensuring stable calibration, we applied first and second different orders of derivatives (Heise and Winzen 2002, Duckworth 2004), with the Savitzky and Golay method (Savitzky and Golay 1964). Finally, models that gave the lowest RMSECV, highest R^2, slope and RPD value were considered to be optimal for future concentration estimates.

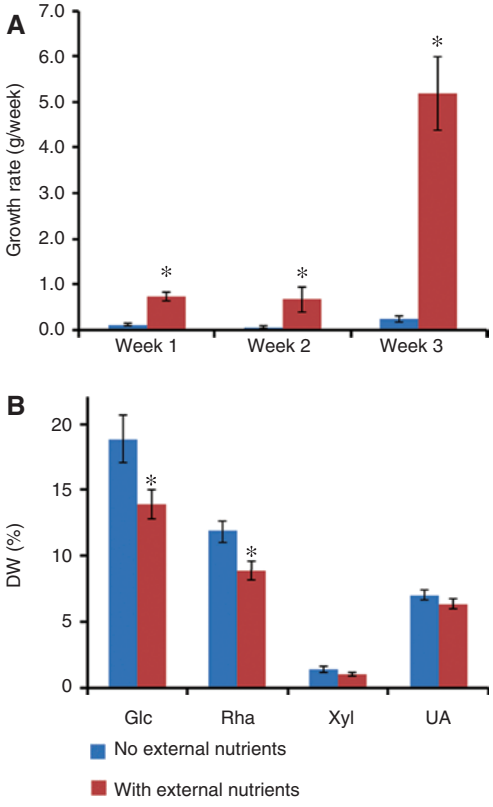

Figure 1: (A) Growth rates of *Ulva fasciata* with and without external nutrient supply. (B) Monosaccharides (glucose, Glc; rhamnose, Rha; xylose, Xyl) and glucuronic acid (UA) content (% of dry weight) in thalli of *Ulva fasciata* grown with and without external nutrients. Results are means (n = 8) ± standard error of means (SEM) and asterisks indicate significant differences ($p < 0.05$) between nutrient treatments.

Results and discussion

External nutrient supply increases biomass growth rate, but decreases monosaccharide content in *Ulva fasciata* thalli

External nutrient supply increased the thallus growth rate (Figure 1A). The growth rate of fertilised thalli was 0.730 ± 0.095 at week 1, 0.676 ± 0.278 at week 2 and 5.186 ± 0.870 g FW week^{-1} at week 3. The growth of thalli without added nutrients was 0.118 ± 0.027 at week 1, 0.063 ± 0.031 at week 2 and 0.240 ± 0.068 g FW week^{-1} during week 3.

We found that adding nutrients decreased ($p < 0.05$) glucose and rhamnose concentrations in *Ulva fasciata* tissues but had no effect on the concentrations of xylose and glucuronic acid (Figure 1B). The contents of rhamnose, glucose, xylose and glucuronic acid in the thalli without external nutrients were 11.93 ± 0.91 mg g^{-1} dry weight (DW), 18.85 ± 1.78 mg g^{-1} DW, 1.42 ± 0.20 mg g^{-1} DW and 7.05 ± 0.40 mg g^{-1} DW, respectively. The contents of rhamnose, glucose, xylose and glucuronic acid in the thalli with external nutrient supply were 8.93 ± 0.73 mg g^{-1} DW, 13.94 ± 1.11 mg g^{-1} DW, 1.08 ± 0.15 mg g^{-1} DW and 6.39 ± 0.39 mg g^{-1} DW, respectively. These results are consistent with previous findings that the C : N ratio in species of *Ulva* reduces under nitrogen-rich conditions

and increases during nitrogen starvation (Pinchetti et al. 1998).

Changes in spectral features between clones of *Ulva* thalli grown with and without external nutrient supply

Generally, vegetation reflectance spectra are quite informative regarding vegetation chlorophyll absorption bands in the VIS (400–700 nm) and NIR (700–1100 nm) and the effects of plant water absorption in the SWIR (1100–2500 nm). Figure 2 shows spectral reflectance variability for thalli grown with and without external nutrient supply (Figure 2; blue vs. red spectrum lines, respectively) for both wet (A) and dry (B) *Ulva fasciata*. Samples differ not only in absorbance depths across a spectrum (due to the presence of chemical chromophors) but also in spectral intensity, curve shape and spectral slopes across the measured spectral range.

The change in absorption depth around 1400 and 1900 nm between dry and wet *U. fasciata* is particularly deep for wet samples. Water has a broad absorption range centred around 1400 and 1940 nm that masks other absorption features associated with constituents such as nitrogen, lignin, sugar and cellulose.

For both wet and dry *U. fasciata* biomass, as shown in Figure 2C and D, several indices and slopes across similar spectral ranges were generated with an aim to distinguish between thalli with and without external nutrient supply. NDIs that separate the samples best lie between the following pairs of wavelengths: 550–686 nm, 425–850 nm and 700–900 nm. In addition, spectral slopes calculated between 470–530 nm and 686–770 nm are efficient for distinguishing between the two groups. Low carbohydrate content (no external nutrients) and high carbohydrate content groups (external nutrient supply) clearly stand out ($p < 0.001$). Importantly, these spectral ranges are not impacted directly by strong water absorbance.

Exploratory assessment of the potential of spectral-based chemometrics of monosaccharide content in *Ulva fasciata*

Table 2 presents the best results obtained for the cross-calibration set based on 16 samples. Several models predicted glucose content efficiently. We found that for

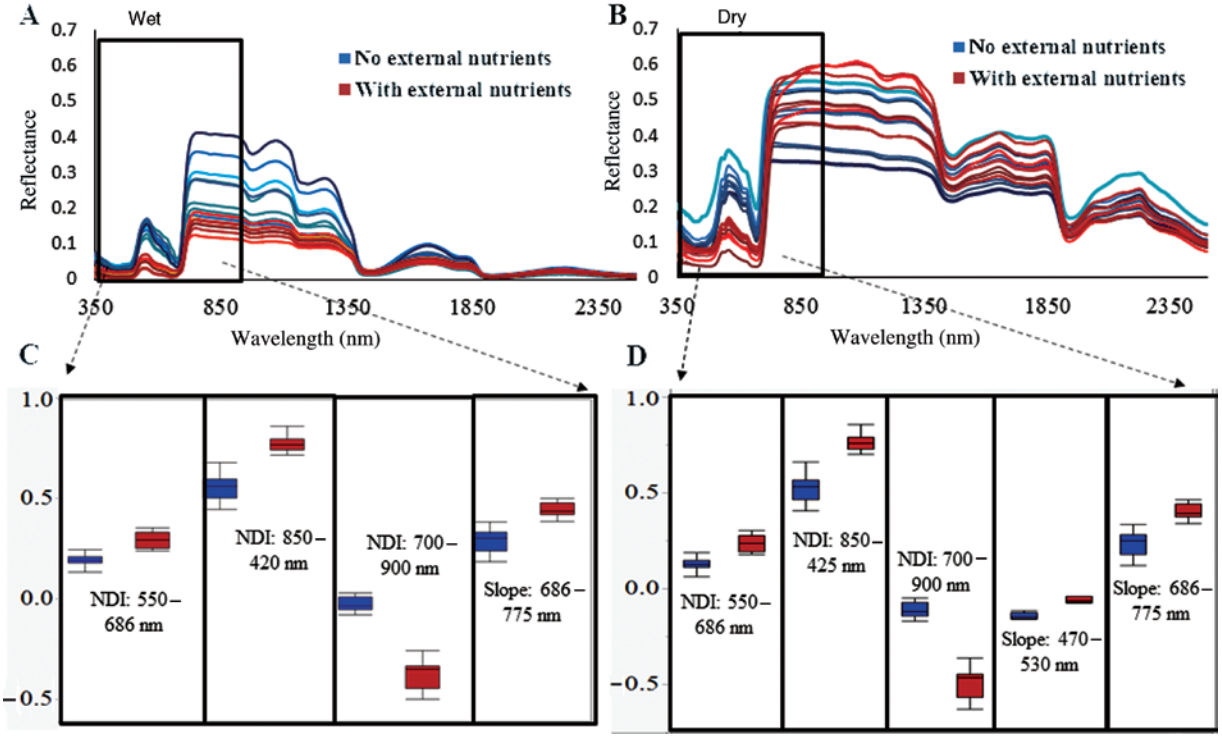

Figure 2: (A–B) Spectral reflectance of wet and dry samples of *Ulva fasciata*. (C–D) Normalised difference spectral reflectance index (NDI) and spectral slope between two wavelengths; note that spectral index differentiates between samples with and without nutrient supply.

Table 2: Statistical parameters obtained for the calibration stage for each of the partial least squares (PLS) regression models to predict carbohydrate concentration in *Ulva fasciata*.

Type of biomass	Type of carbohydrate	Transformation of concentration	Model	#LV	RMSECV	R^2	Slope	RPD
Dry *Ulva fasciata*	Glucose	Log	2deriv + smoothing Run on 28 wavelengths	5	0.02 (1.1)[a]	0.88	0.90	3.3
	Glucose	None	Reflectance Run on 25 wavelengths	7	2.0	0.86	0.98	1.8
	Rhamnose	Log	Norm + smoothing Run on 20 wavelengths	5	0.06 (1.14)[a]	0.82	0.99	2.0
	Xylose	Log	2deriv + smoothing Run on 12 wavelengths		0.1 (1.3)[a]	0.80	0.85	1.5
	Glucuronic acid		No accurate model was found					
Wet *Ulva fasciata*	Glucose	Log	2deriv + smoothing Run on 36 wavelengths	3	0.04	0.81	0.89	2.3
	Glucose	None	Slope model (9 slopes)	2	3.1	0.78	0.81	1.7
	Rhamnose	None	2deriv + smoothing Run on 40 wavelengths	3	3.5	0.70	0.75	1.9
	Xylose		No accurate model found					
	Glucuronic acid	None	2deriv + smoothing Run on 44 wavelengths	3	3.3	0.83	0.83	2.2

RMSECV, root-mean-square error of cross-validation; RPD, ratio of prediction to deviation; #LV, number of LV components (regression coefficients) used to construct the PLS model; R^2 and Slope, coefficient of determination and slope (in original values) of the model.
The following models were considered: 2deriv + smoothing (with different number of wavelengths) (reflectance, considered as the second derivative, followed by a smoothing function and run on selected wavelengths); norm + smoothing (normalisation of spectral reflectance followed by a smoothing function and run on selected wavelengths); slopes; reflectance (run on selected wavelengths).
[a]Indicates inverse log value used, with original concentration values in parentheses. Carbohydrate concentrations were log-transformed in order to get a normal distribution of the *Y* variable in PLS model.

prediction of different sugar components based on spectral measurements, the resulting quality is strongly dependent on the wavelength selection. This supervised model provides better results than when using the entire spectrum. During the selected cross-validation modelling, significant improvement in predictive accuracy, lower value of RMSECV, higher RPD and R^2 values was achieved when all pre-processed models were reassessed on a reduced number of spectral variables (according to Martens test; Esbensen 2002). Due to the limited number of samples (e.g. limited dynamic range of reference values), *Y* values (concentrations) for several models were log-transformed to get a normal distribution.

Figure 3A shows measured vs. predicted glucose content obtained for the best-fit model for dry biomass. The linear plot exhibits a slope of 0.87 and $R^2 = 0.88$. A much clearer picture of spectroscopically determined glucose content changes compared with original reflectance is obtained from the plot of factor loadings [loading vectors (LV), or regression coefficients] vs. wavelength (Figure 3B). The first three LV components in the PLS model explained 95% of the *X* variance (spectra) and 90% of the *Y* variance (glucose content). This indicated that most of the spectral variation that was modelled by PLS is related to the glucose content.

Figure 3C shows the X-(PC1) and Y-(PC2) scores of a PLS regression plot of samples from the PLS model for glucose content for dry samples. The score plot indicated that a significant part of the spectral variations observed in the dry samples are indeed related to glucose as predicted by the PLS model. Specifically, there was an increasing trend in glucose content among samples from the bottom to the top along PC2, following a slight diagonal, presumably due to the difference in water content. Furthermore, there is a separation between the two groups of samples along PC1, samples with no external nutrient supply are located on the left of the score plot, whereas samples with external nutrient supplies are located on the right of the plot.

Figure 4 shows the best-fit model results for wet biomass. Similar to dry biomass, the best pre-processing technique was to consider reflectance as the second derivative, followed by a smoothing function and to run for selected wavelengths. Here we used the Savitzky-Golay smoothing method to reduce high-frequency noise. This is an averaging algorithm that fits a polynomial to the data points. The relatively high predictive ability at the

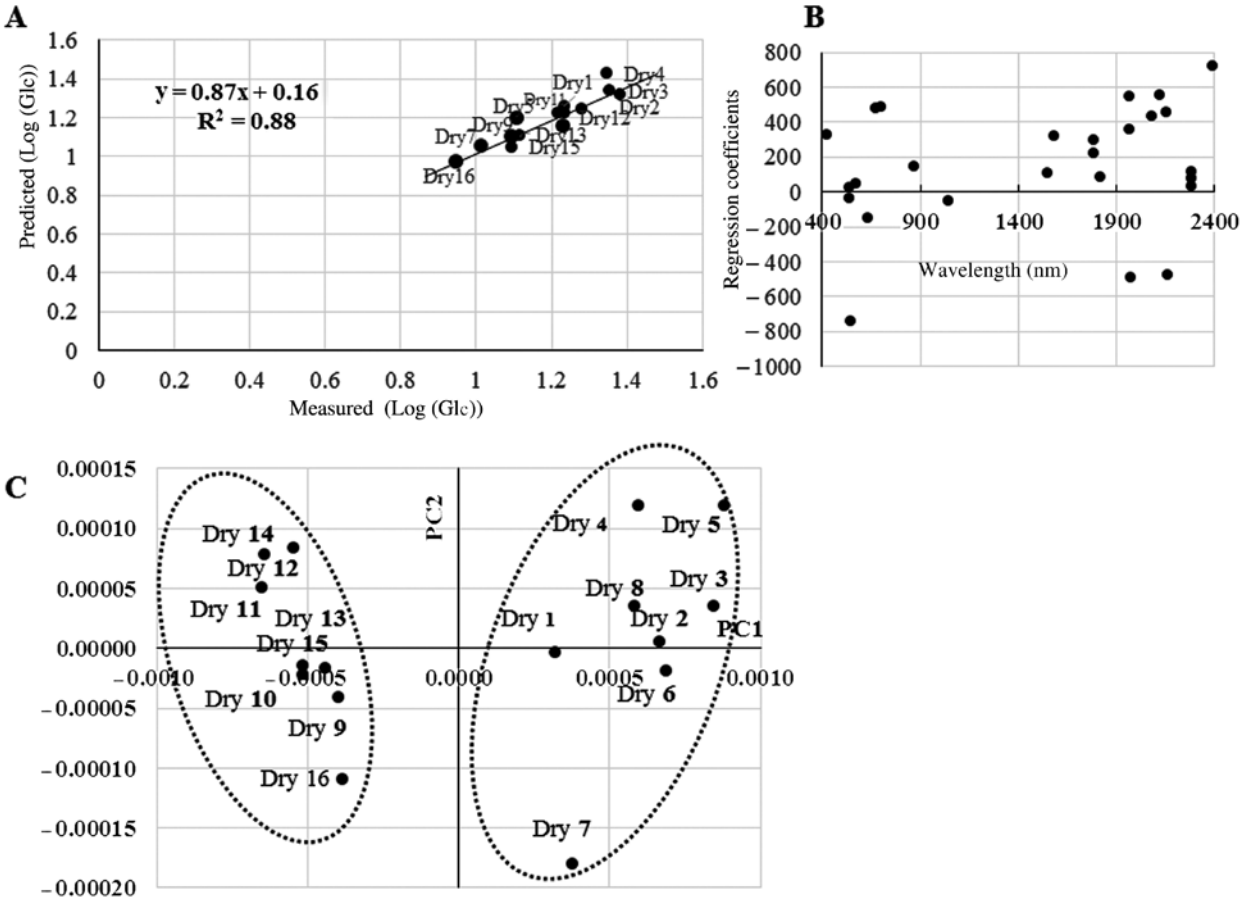

Figure 3: (A) Measured (n = 16) vs. predicted glucose content (% of dry weight) for dry *Ulva fasciata* obtained for the best-fit model (second derivative of reflectance spectra when applied on selected wavelengths). (B) Partial least squares loadings vectors (LV1–3) for the optimal calibration model as calculated for glucose content using dry samples data set. (C) Score plot for the partial least squares best-fit model for glucose content using dry samples. Note the separation between samples with external nutrient supply (denoted as dry 9–dry 16, located on the left side of the score plot) and those without nutrient supply (denoted as dry 1–dry 8, located on the right side of the plot) as evident from the score plot.

cross-validation set level enables us to propose that our PLS models can be used to predict glucose content precisely. The highest regression coefficients were for the spectral range 1100–1300 nm (Figure 4B), which probably relates to the presence of sugar, starch and cellulose (Curran 1989).

Furthermore, as is evident from the analyses of the score plot of the wet biomass data set (Figure 4C), there is a separation between the two groups of samples along PC1, samples with no external nutrients are located on the left of the score plot, whereas samples with external nutrients are on the right. Similar to the dry model (Figure 3C), there is an increasing trend in glucose content among samples from the bottom to the top along PC2.

The major limitation of the current study is the relatively small number of samples used, which limits the PLS model. This limitation, however, does not change our main findings that spectral reflectance depends on glucose content. Importantly, this dependence is apparent for both dry and wet *Ulva fasciata* biomass. In addition, the same spectra and similar modelling approaches could be used in further studies for quantification of other important biorefinery constituents of *Ulva* biomass, such as starch, proteins, pigments and special chemicals. For example, Lugassi et al. (2015b) concluded that crude protein and neutral detergent fibre contents could be predicted using the spectral slope method for dry and wet vegetation.

Conclusions

This study shows that the change in spectral slope can be used in rapid phenotyping of *Ulva fasciata* as an indicator for high glucose content. Glucose is the most promising

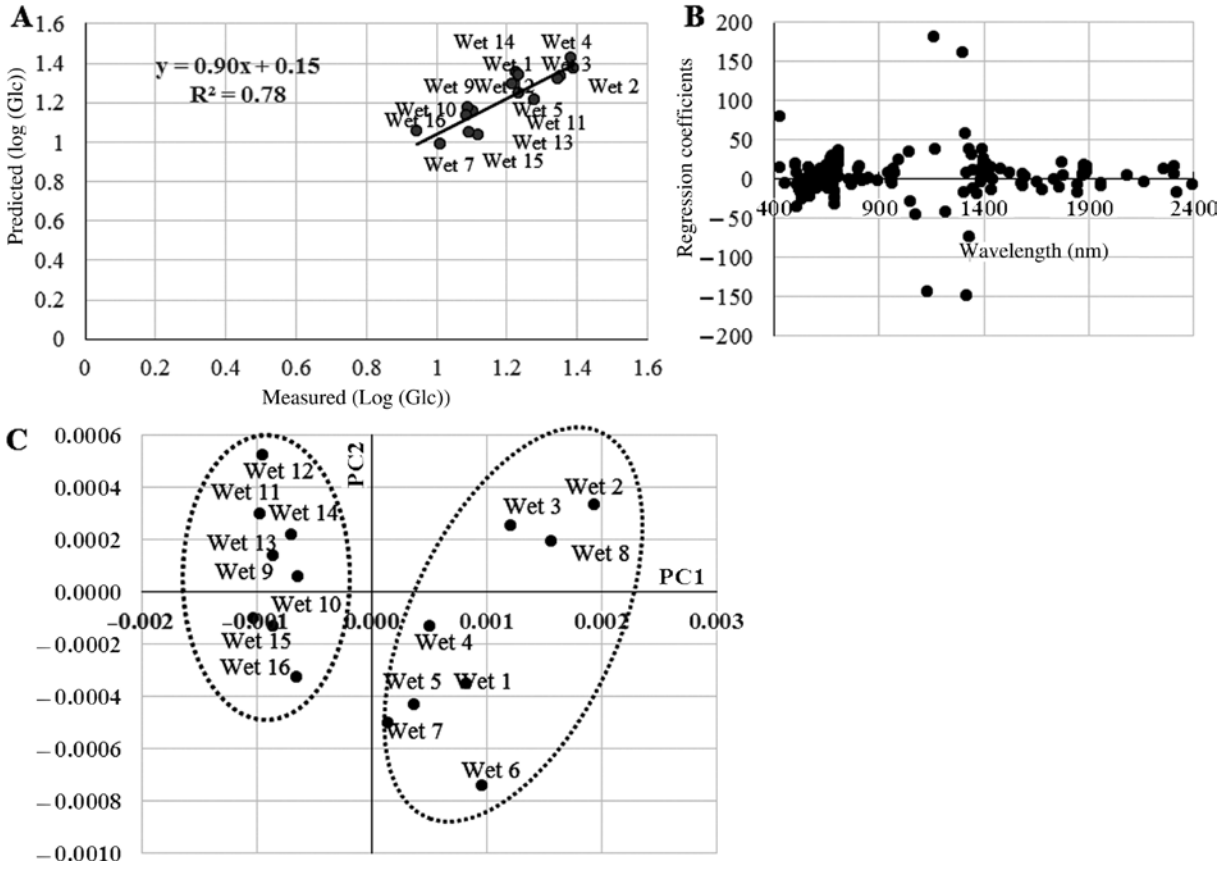

Figure 4: (A) Measured (n = 16) vs. predicted glucose content (% of dry weight) for wet *Ulva fasciata* obtained for the best-fit model (second derivative of reflectance spectra when applied on selected wavelengths). (B) Partial least squares loadings vectors (LV1–3) for the optimal calibration model as calculated for glucose content using wet samples data set. (C) Score plot for the partial least squares best-fit model for glucose content using wet samples. Note the separation between samples with nutrient supply (denoted as wet 9–wet 16, located on the left side of the score plot) and those without nutrient supply (denoted as wet 1–wet 8, located on the right side of the plot) as evident from the score plot.

source for fermentation and production of sustainable chemicals and biofuels. We have shown that it is possible to discriminate between high and low contents of glucose, rhamnose, xylose and glucuronic acid for both dry and wet samples of *U. fasciata* using similar spectral ranges across visible and near-infrared wavelengths. This result is important for the development of a future field device intended for rapid macroalgal profiling for breeding and strain development for marine biorefineries. As an example, we estimated the content of major monosaccharides of *U. fasciata* using PLS analyses based on spectral reflectance measurements. We found that the wavelength range of NIR-SWIR spectra for calibration and/or prediction affect the reliability of NIRS analysis. This study should be expanded to a larger calibration set of values.

Acknowledgments: The authors acknowledge the TAU Center for Innovation in Transportation and The Israel Ministry of National Infrastructures, Energy and Water Resources for support. The authors acknowledge and appreciate Prof. Matthew J. Dring's scientific comments.

References

Aitken, D., C. Bulboa, A. Godoy-Faundez, J.L. Turrion-Gomez and B. Antizar-Ladislao. 2014. Life cycle assessment of macroalgae cultivation and processing for biofuel production. *J. Clean. Prod. 75*: 45–56.

Blanco, M. and I. Villarroya. 2002. NIR spectroscopy: a rapid-response analytical tool. *Trac-Trend. Anal. Chem. 21*: 240–250.

Bruhn, A., J. Dahl, H.B. Nielsen, L. Nikolaisen, M.B. Rasmussen, S. Markager, B. Olesen, C. Arias and P.D. Jensen. 2011. Bioenergy potential of Ulva lactuca: biomass yield, methane production and combustion. *Bioresour. Technol. 102*: 2595–2604.

Cabrera-Bosquet, L., J. Crossa, J. von Zitzewitz, M.D. Serret and J. Luis Araus. 2012. High-throughput phenotyping and genomic selection: the frontiers of crop breeding converge. *J. Integr. Plant. Biol. 54*: 312–320.

Curran, P.J. 1989. Remote sensing of foliar chemistry. *Remote Sens. Environ. 30*: 271–278.

Duckworth, J. 2004. Mathematical data processing. *In:* (C.A. Roberts, J. Workman Jr., J.B. Reeves III, eds.) *Near-infrared spectroscopy in agriculture*. ASA-CSSA-SSSA, Madison. pp. 115–132.

Esbensen, K. 2002. *Multivariable data analysis in practice*. 5th edition. Camo Process AS, Oslo.

Gerbens-Leenes, W., A.Y. Hoekstra and T.H. van der Meer. 2009. The water footprint of bioenergy. *Proc. Natl. Acad. Sci. U. S. A. 106*: 10219–10223.

Golberg, A., E. Vitkin, G. Linshiz, S.A. Khan, N.J. Hillson, Z. Yakhini and M.L. Yarmush. 2014. Proposed design of distributed macroalgal biorefineries: thermodynamics, bioconversion technology, and sustainability implications for developing economies. *Biofuels. Bioprod. Biorefining 8*: 67–82.

Hannon, M., J. Gimpel, M. Tran, B. Rasala and S. Mayfield. 2010. Biofuels from algae: challenges and potential. *Biofuels 1*: 763–784.

Heise, H. and R. Winzen. 2002. Fundamental chemometric methods. *In:* (H. Siesler, Y. Ozaki, S. Kawata and H. Heise, eds.) *Near-infrared spectroscopy spectroscopy: principles, instruments and applications*. WILEY-VCH, pp. 125–160. ISBN: 978-3-527-61267-3.

Jiao, Q. and Q. Liu. 1999. Simple spectrophotometric method for the estimation of algal polysaccharide concentrations. *J. Agric. Food Chem. 47*: 996–998.

Korzen, L., I.N. Pulidindi, A. Israel, A. Abelson and A. Gedanken. 2015a. Single step production of bioethanol from the seaweed Ulva rigida using sonication *RSC Adv. 5*: 16223–16229.

Korzen, L., I.N. Pulidindi, A. Israel, A. Abelson and A. Gedanken. 2015b. Marine integrated culture of carbohydrate rich Ulva rigida for enhanced production of bioethanol. *RSC Adv. 5*: 59251–59256.

Kraan, S. 2013. Mass cultivation of carbohydrate rich microalgae, a possible solution for sustainable biofuel production. *Mitig. Adapt. Strateg. Glob. Change. 18*: 27–46.

Li, L., Q. Zhang and D.A. Huang. 2014. Review of imaging techniques for plant phenotyping. *Sensors 14*: 20078–20111.

Lugassi, R., A. Chudnovsky, E. Zaady, L. Dvash and N. Goldshleger. 2015a. Spectral slope as an indicator of pasture quality. *Rem. Sens. 7*: 256–274.

Lugassi, R., A. Chudnovsky, E. Zaady, L. Dvash and N. Goldshleger. 2015b. Estimating pasture quality of fresh vegetation based on spectral slope of mixed data of dry and fresh vegetation-method development. *Rem. Sens. 7*: 8045–8066.

Mark, H. 2000. Quantitative spectroscopic calibration. *In*: (R.A. Meyers, ed.) *Encyclopedia of analytical chemistry: applications, theory, and instrumentation*. John Wiley & Sons Ltd, Chichester.

Mouazen, A.M., W. Saeys, J. Xing, J. De Baerdemaeker and H. Ramon. 2005. Near infrared spectroscopy for agricultural materials: an instrument comparison. *JNIRS 13*: 87–97.

Mutka, A.M. and R.S. Bart. 2015. Image-based phenotyping of plant disease symptoms. *Front. Plant Sci. 5*: 734.

Pinchetti, J.L.G., E. del Campo Fernández and P. Moreno Diez. 1998. Nitrogen availability influences the biochemical composition and photosynthesis of tank-cultivated Ulva rigida (Chlorophyta). *J. Appl. Phycol. 10*: 383–389.

Ramsey, E.A., M.S. Rangoonwala, A. Thomsen and A. Schwarzschild. 2002a. Spectral definition of the macro-algae Ulva curvata in the back-barrier bays of the Eastern Shore of Virginia, USA. *Int. J. Remote Sens. 33*: 586–603.

Ramsey, E., A. Rangoonwala, M.S. Thomsen and A. Schwarzschild. 2002b. Flat-plate techniques for measuring reflectance of macro-algae (*Ulva curvata*). *Int. J. Remote Sens. 33*: 3147–3155.

Robic, A., D. Bertrand, J.F. Sassi, Y. Lerat and M. Lahaye. 2009. Determination of the chemical composition of ulvan, a cell wall polysaccharide from Ulva spp. (Ulvales, Chlorophyta) by FT-IR and chemometrics. *J. Appl. Phycol. 21*: 451–456.

Robinson, N., P. Winberg and L. Kirkendale. 2012. Genetic improvement of macroalgae: status to date and needs for the future. *J. Appl. Phycol. 25*: 703–716.

Savitzky, A. and M.J.E. Golay. 1964. Smoothing and differentiation of data by simplified least squares procedures. *Anal. Chem. 36*: 1627–1639.

van der Wal, H., B.L. Sperber, B. Houweling-Tan, R.R. Bakker, W. Brandenburg and A.M. López-Contreras. 2013. Production of acetone, butanol, and ethanol from biomass of the green seaweed Ulva lactuca. *Bioresour. Technol. 128*: 431–437.

Viscarra Rossel, R.A. 2007. Robust modelling of soil diffuse reflectance spectra by bagging-partial least squares regression. *JNIRS 15*: 39–47.

Vitkin, E., A. Golberg and Z. Yakhini. 2015. BioLEGO – a web-based application for biorefinery design and evaluation of serial biomass fermentation. *Technol. 3:* 1–10.

Walter, A., F. Liebisch and A. Hund. 2015. Plant phenotyping: from bean weighing to image analysis. *Plant Methods 11*: 14.

Wargacki, A.J., E. Leonard, M.N. Win, D.D. Regitsky, C.N. Santos, P.B. Kim, S.R. Cooper, R.M. Raisner, A. Herman, A.B. Sivitz, A. Lakshmanaswamy, Y. Kashiyama, D. Baker and Y. Yoshikuni. 2012. An engineered microbial platform for direct biofuel production from brown macroalgae. *Science 335*: 308–313.

Williams, P.C. and K. Norris. 2001. Method development and implementation of near-infrared spectroscopy in industrial manufacturing processes. *In*: *Near-Infrared Technology in the Agricultural and Food Industries*. 2nd edition. American Association of Cereal Chemists, St. Paul, MN.

Bionotes

Shai Shefer
Porter School of Environmental Studies, Tel Aviv University, Israel

Shai Shefer is currently an MSc student at Tel Aviv University, Porter School of Environmental Studies, focusing on macroalgae profiling for breeding and strain development for marine biorefinery methods. He completed his MBA at the College of Management Academic Studies and BSc at the Hebrew University of Jerusalem.

Alvaro Israel
Israel Oceanographic and Limnological Research Ltd. Haifa, Israel

Alvaro Israel is currently a senior scientist at the Israel Oceanographic and Limnological Research Institute at Haifa, Israel, and has been engaged for over 20 years in the study of seaweed biology and ecology. He has been involved in projects related to carbon fixation, photosynthesis, taxonomy and applied phycology.

Alexander Golberg
Porter School of Environmental Studies, Tel Aviv University, Israel

Alexander Golberg is currently a faculty member at Tel Aviv University, Porter School of Environmental Studies. He completed his PhD in bioengineering at the Hebrew University of Jerusalem, focusing on low-cost bioenergy technologies for low-income countries. He continued working on a variety of projects that involved engineering and biology at UC Berkeley and Harvard Medical School. In 2012, he won the Green Talent 2012 Award for the design of distributed marine biorefineries for the production of feed and transportation fuels for rural areas in low-income counties. His main research interests are in bioenergy conversion efficiency and bioprocess development.

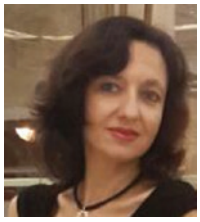

Alexandra Chudnovsky
Department of Geography and Human Environment, Tel Aviv University, Zalig Street 10, Ramat Aviv, Tel Aviv 69978, Israel,
achudnov@post.tau.ac.il

Alexandra Chudnovsky is currently a faculty member at Tel Aviv University, Department of Geography and Human Environment, School of Geosciences and a visiting Scientist at the Harvard T.H. Chan School of Public Health. Much of her research is concerned with developing modeling methods to predict and evaluate the contribution of local and regional pollution sources to urban air, water, vegetation and soil quality using passive remote-sensing technologies.